

# A Distributed Localization Scheme for Wireless Sensor Networks with Improved Grid-Scan and Vector-Based Refinement

Jang-Ping Sheu, *Senior Member, IEEE*, Pei-Chun Chen, and Chih-Shun Hsu

**Abstract**—Localization is a fundamental and essential issue for wireless sensor networks (WSNs). Existing localization algorithms can be categorized as either range-based or range-free schemes. Range-based schemes are not suitable for WSNs because of their irregularity of radio propagation and their cost of additional devices. In contrast, range-free schemes do not need to use received signal strength to estimate distances. They only need simple and cheap hardware and are, thus, more suitable for WSNs. However, existing range-free schemes are too costly and not accurate enough or are not scalable. To improve previous works, we present a fully distributed range-free localization scheme for WSNs. We assume that only a few sensor nodes, called anchors, know their locations, and the remaining (normal) nodes need to estimate their own locations by gathering nearby neighboring information. We propose an improved grid-scan algorithm to find the estimated locations of the normal nodes. Furthermore, we derive a vector-based refinement scheme to improve the accuracy of the estimated locations. Analysis, simulation, and experimental results show that our scheme outperforms the other range-free schemes even when the communication radius is irregular.

**Index Terms**—Anchor nodes, localization, range based, range-free, wireless sensor networks.

## 1 INTRODUCTION

LOCALIZATION is a fundamental and essential issue for wireless sensor networks (WSNs). Many of the applications and communication protocols of WSNs are based on the location information of sensor nodes, such as calculating the coverage of WSNs, tracking the location of events and intruders, geographic-based routing, and geocasting [13], [18], [19]. Since a WSN usually consists of thousands of low-cost sensor nodes, it is not practical to equip each sensor node with a positioning device such as the Global Positioning System (GPS) [10], [17]. The more reasonable solution is to assume that only a small portion of sensor nodes (called anchors) obtain their location information via GPS or the system administrator, and the remaining nodes without location information (called normal nodes) can estimate their locations according to the location information of the anchors.

Many localization algorithms for WSNs have been proposed recently. These localization algorithms for WSNs can be categorized as either range-based or range-free schemes. The range-based scheme determines the distance between two different sensor nodes based on a variety of information, such as Time of Arrival (TOA) [18], Time Difference of Arrival (TDOA) [2], Angle of Arrival (AOA) [1],

and Received Signal Strength Indicator (RSSI) [16]. After the distance has been determined, the location can be estimated according to the distance information. The estimation of the above time-of-flight technologies can be affected by multipath and noise. Moreover, these schemes often need to be equipped with additional hardware. Consequently, range-based schemes are impractical solutions for the resource-limited WSNs.

Because of the drawbacks of ranged-based schemes, many range-free localization schemes have been proposed, such as Centroid [8], APIT [13], DV-HOP [10], CPE [14], DLE [20], MCL [21], MSL [22], and UPL [25]. In ranged-free schemes, the sensor nodes without location information (called normal nodes) gather location information from nodes with known locations (called anchors) and estimate their own locations according to the location information of the anchors. However, existing ranged-free schemes are either too costly (cause heavy traffic load), not accurate enough, or not scalable.

To improve previous works, we propose a Distributed Range-Free Localization Scheme (DRLS) for static WSNs. In the proposed scheme, each node gathers the nearby anchors' locations and then estimates its own location. We propose an improved grid-scan algorithm, whose computation cost is lower than the original grid-scan algorithm [13], to calculate the estimated locations of the normal nodes. Furthermore, we derive a vector-based refinement scheme to improve the accuracy of the estimated locations. The estimated location is refined according to the combined vectors formed by the target node (the normal node that is currently estimating its location) and farther anchors. A farther anchor is defined as the anchor that does not cover the target node but covers the target node's estimative region. Analysis, simulation, and experimental results show

• J.-P. Sheu is with the Department of Computer Science, National Tsing Hua University, 101, Sec. 2, Kuang-Fu Road, Hsinchu 30013, Taiwan, R.O.C. E-mail: sheupp@cs.nthu.edu.tw.

• P.-C. Chen is with the Department of Computer Science and Information Engineering, National Central University, Chung-Li 320, Taiwan, R.O.C.

• C.-S. Hsu is with the Department of Information Management, Shih Hsin University, Taipei 116, Taiwan, R.O.C. E-mail: cshsu@cc.shu.edu.tw.

Manuscript received 22 Oct. 2006; revised 8 Nov. 2007; accepted 27 Jan. 2008; published online 27 Feb. 2008.

For information on obtaining reprints of this article, please send e-mail to: [tmc@computer.org](mailto:tmc@computer.org), and reference IEEECS Log Number TMC-0288-1006.

Digital Object Identifier no. 10.1109/TMC.2008.35.

that the proposed algorithm can improve the accuracy of the estimated location.

The rest of the paper is organized as follows: Section 2 reviews some related works on localization. Section 3 describes our DRLS. Performance evaluation is shown in Section 4. Conclusions are made in Section 5.

## 2 RELATED WORK

Many localization algorithms have been proposed recently [1], [2], [3], [4], [5], [6], [7], [8], [9], [10], [11], [12], [13], [14], [15], [16], [20], [21], [22], [23], [24], [25], [26]. The localization algorithms can be classified into two categories, namely, range-based and range-free schemes. The details of the two schemes are shown as follows.

### 2.1 Range-Based Localization Schemes

The range-based localization schemes can be further classified into TOA, TDOA, AOA, and RSSI measurements based on the way they acquire distance information. TOA measurement is commonly used to obtain range information between two communicating nodes according to the measurement of signal propagation time. The most basic position system used in TOA measurement is GPS [18]. TDOA measurement is similar to TOA in that they both require expensive hardware and use the signal propagation time to derive range information. However, TDOA uses ultrasound signals to help sensor nodes acquire distance information. TDOA has been widely adopted by several localization schemes in WSNs, such as the Cricket Location-Support System [2]. In the Cricket system, the beacon nodes periodically broadcast position information over RF and ultrasound signals concurrently. A normal node will receive the RF signal earlier than the ultrasound signal and, afterward, calculates the time difference between the arrival time of the RF signal and the ultrasound signal. The distance measurement between the normal node and the beacon node can then be determined. Measurements based on the signal propagation time can be affected by multipath fading and noise interference. Therefore, TOA and TDOA are impractical solutions for WSNs.

AOA measurement estimates the relative angles between neighbors. However, AOA measurement requires additional expensive hardware, such as a directional antenna or a digital compass [11]. Consequently, AOA measurement is not suitable for resource-limited WSNs.

RSSI is another approach based on the relation between signal strength and distance. RADAR [16] is one of the schemes adopting RSSI. Based on the radio propagation theory, RSSI converts the received signal strength to the distance between receiving nodes and transmitting nodes. The formula of the radio propagation theory is composed of the transmitted power, the received power, and the path loss. However, problems of multipath fading, unstable signal propagation, and background noise make the distance derived from RSSI inaccurate. The other works related to range-based schemes can be found in [24], [25], and [26].

### 2.2 Range-Free Localization Schemes

Because of the drawbacks of ranged-based schemes, many range-free solutions have been proposed. In the Centroid

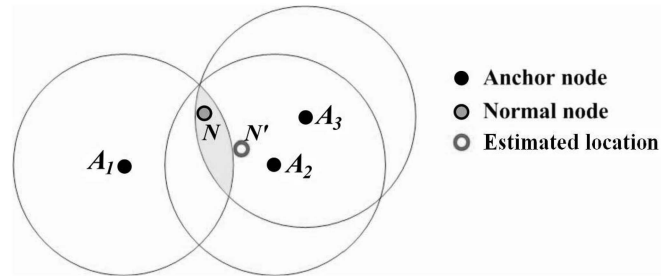


Fig. 1. The estimated location derived from the Centroid algorithm.

algorithm [8], normal nodes collect location information from their neighboring anchors and calculate their estimated locations by using the Centroid formula. The Centroid algorithm is simple and can get accurate estimated location when the anchor ratio is high or the distribution of anchors is regular. However, when the anchor ratio is low or the distribution of anchors is not even, the estimated location derived from the Centroid algorithm tends to be inaccurate. In Fig. 1, the shaded region is the overlapping communication region of three anchors, namely,  $A_1$ ,  $A_2$ , and  $A_3$ . If normal node  $N$  can receive beacons from neighboring anchors  $A_1$ ,  $A_2$ , and  $A_3$ , it is rational for  $N$  to regard the center of the shaded region as its own estimated location. However, when using the Centroid algorithm, the estimated location (denoted as  $N'$ ) of the normal node  $N$  is the average of the coordinates of nodes  $A_1$ ,  $A_2$ , and  $A_3$ , which is obviously outside the overlapping communication region.

Another range-free localization scheme, named APIT, is proposed in [13]. By using beacons from neighboring anchors, APIT repeats an area-based approach called the Point-In-Triangulation (PIT) test with different combinations of neighboring anchors to narrow down the normal node's estimative region. After the PIT test, the APIT utilizes a grid-scan algorithm to derive the intersection region of all the triangles and regards the center of the intersection region as the estimated location of the normal node. It is shown that the APIT scheme can achieve an acceptable localization error when the anchor ratio is high and the communication overhead is as low as the Centroid algorithm's. However, in APIT, the network area is divided into many small square grids. The grid-scan algorithm needs to scan these grids and judge if the square grid is in the triangle region formed by the connected lines between near anchors. The memory required to store the value of the grid array is large, and since the sensor node has only a small memory, APIT is not suitable for WSNs.

Based on the concept of distance vector (DV) routing, DV-HOP is proposed in [10]. The anchors broadcast their location package throughout the network. Other anchors can obtain the minimum hop count to each anchor. Each anchor can convert the hop count to physical distance and broadcast the estimated average distance per hop to neighboring normal nodes. Normal nodes can then calculate their locations based on the received anchor's location, the hop count from the anchor, and the average per hop distance.

The Convex Position Estimation (CPE) algorithm [14] uses convex optimization to estimate the position of the sensor node. If a normal node can communicate with some neighboring anchors, it means that there are connectivity

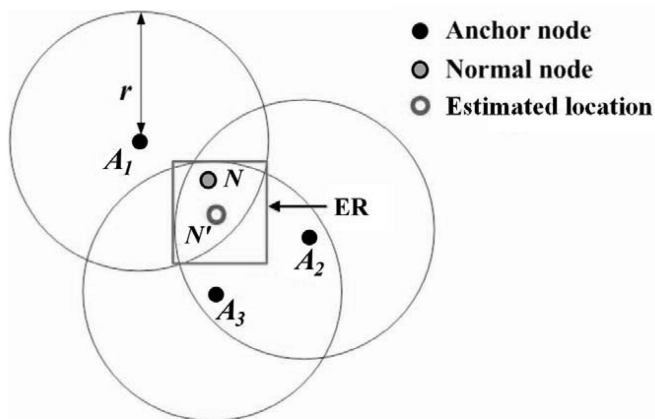


Fig. 2. The estimated location derived by the CPE algorithm.

constraints between the normal node and its neighboring anchors. Since the location of the normal node must be within the intersection of the communication regions of these anchors, information such as locations and communication ranges of these nearby anchors can be used to estimate the location of the normal node. Aside from this, for the ease of calculating, the CPE algorithm defines the estimative rectangle (ER), which bounds the overlapping region and regards the center of the rectangle as the estimated location of the normal node. The four sides of the ER are parallel to the  $x$ -axis and the  $y$ -axis. For example, in Fig. 2, the normal node  $N$  is within the communication range  $r$  of three neighboring anchors, namely,  $A_1$ ,  $A_2$ , and  $A_3$ . That is, there are connectivity constraints between the normal node  $N$  and its neighboring anchors  $A_1$ ,  $A_2$ , and  $A_3$ . By using combinations of these connectivity constraints, the ER of the overlapping region, where a normal node  $N$  resides, can be calculated. Finally, the node  $N'$ , which is the center of the ER, is the estimated location of the normal node  $N$ . The CPE algorithm is a centralized localization scheme since each normal node sends the collected connectivity constraints back to a centralized controller. The centralized controller then estimates the location of every normal node and floods the estimated location back to every normal node. Thus, the global solution can be acquired. However, the traffic load is heavy, and the CPE algorithm scales poorly when the network is large.

The CPE algorithm [14] has also been improved in a distributed version in [15]. In this distributed algorithm, normal nodes improve their estimated locations by incorporating connectivity constraints, as well as constraints imposed by a moving target. The normal nodes acquire an initial estimated location by using connectivity constraints and then use detection or nondetection of a moving target to update their estimated locations. In reality, it is difficult to move a target successfully in large-scale WSNs, and constraints imposed by the moving target cannot be acquired. Thus, this distributed algorithm scales poorly because of the size of the WSNs.

In the Distributed Location Estimating (DLE) algorithm [20], each node without location information only needs to collect the location information of neighboring nodes and then calculate the ER to estimate its location. Aside from this, DLE uses some rules to adjust the estimative region

according to the relative locations of the normal nodes and the farther beacon nodes. Thus, the accuracy of the normal node's estimative region can be improved by discarding the communication area of the beacon node (called the farther beacon node), which does not cover the normal node, from the original estimative region. However, the rules used to adjust the estimative region sometimes overdiscards the communication area, which does not cover the normal node and can lead to an estimative error when calculating the estimated location. The range-free localization schemes for WSNs with mobile nodes can be found in [21], [22], and [23].

### 2.3 Motivation and Contributions

To improve the localization accuracy and to lower the computation cost of previous works, we propose a DRLS for WSNs. The contributions of the proposed scheme are shown as follows:

- Different from APIT, in DRLS, each normal node gathers two-hop information during the beacon exchange phase so that it can collect both positive and negative connectivity constraints to refine its estimated location. Since each normal node only uses local information to estimate its own location, DRLS is scalable.
- The grid-scan phase of DRLS combines the ideas of ER and grid scan so that we can not only improve the accuracy of the estimated location, but also greatly reduce the grid-scan costs. We believe that no one has ever combined the ideas of ER and grid scan.
- Many existing range-free algorithms use connectivity constraints to estimate location. However, converting the connectivity constraints into vector and using the resultant of the vectors to refine the estimated location are novel ideas. We believe that these ideas have not been proposed before.

## 3 DISTRIBUTE RANGE-FREE LOCALIZATION SCHEME

The DRLS is designed for a WSN whose sensor nodes are randomly deployed in a squared region, wherein every sensor node has a unique ID. Once a sensor node is deployed, it will no longer change its location. In the DRLS, we assume that only a small percentage of sensor nodes, called anchors, get their own location information via GPS or some other mechanism. The other nodes without location information are called normal nodes. By collecting beacons from anchors, DRLS uses the combinations of connectivity constraints gathered from anchors to reduce the scope of the estimative region in which a normal node resides. An improved grid-scan algorithm is then used to derive a more accurate estimated location. Finally, a vector-based refinement scheme is used to further improve the accuracy of the estimated location. There are three phases in the DRLS algorithm. In the first phase, each sensor node exchanges beacons so as to collect connectivity constraints. In the second phase, each normal node uses the improved grid-scan algorithm to get its initial estimated location. In the third phase, the normal node uses the vector-based refinement scheme to improve the accuracy of its estimated

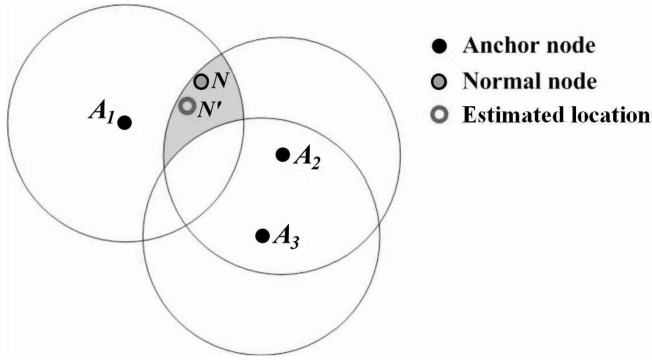


Fig. 3. The impact of the farther anchor.

location. The detailed description of each phase is shown in the following sections.

### 3.1 Beacon Exchange

In the first phase, every anchor gathers the ID and location information of anchors within two hops via two-hop flooding and then broadcasts the collected information to normal nodes within one hop. We will explain why the anchors need to gather the information of other anchors (including ID and location) within two hops using the following examples. In Fig. 3, the normal node  $N$  is within the intersection of the communication regions of anchors  $A_1$  and  $A_2$ . We name anchors  $A_1$  and  $A_2$  as the near anchors of the normal node  $N$ , and we regard the center of the intersection as the initial estimated location of the normal node  $N$ . On the other hand, anchor  $A_3$ 's communication region does not cover node  $N$  but covers the intersection of the communication regions of anchors  $A_1$  and  $A_2$ . Anchor  $A_3$  is named as the farther anchor of the normal node  $N$ . As shown in Fig. 3, the shaded region, which is derived by discarding anchor  $A_3$ 's communication region from the intersection of anchors  $A_1$  and  $A_2$ 's communication regions, is the region where node  $N$  may reside. To derive a more accurate estimated location, node  $N$  needs to gather not only the information (including ID and location) of near anchors  $A_1$  and  $A_2$ , but also the information of the farther anchor  $A_3$ , so that it can further refine its estimated location according to the relative location of the farther anchor and the near anchors' overlapping communication region.

In Fig. 4,  $N$  is the normal node.  $A_1$  and  $A_2$  are the farther and near anchors of node  $N$ , respectively. The farthest possible distance between the farther anchor  $A_1$  and the near anchor  $A_2$  is no more than twice the communication range ( $2r$ ), as shown in Fig. 4. By two-hop flooding, each normal node can collect the location information of near anchors and farther anchors from the near anchors and, thus, improve the accuracy of the estimated location. As the farther anchor is closer to the normal node, it has greater impact on location estimation.

Fig. 5 shows the detail of the beacon exchange via two-hop flooding. Three normal nodes and four anchors are shown in Fig. 5. For the ease of explanation, we will show how the normal node  $N_1$  collects the location information from both near anchors and farther anchors via two-hop flooding.  $A_2$  is the near anchor, and  $A_1$  and  $A_3$  are the farther anchors of the normal node  $N_1$ . Since the distance

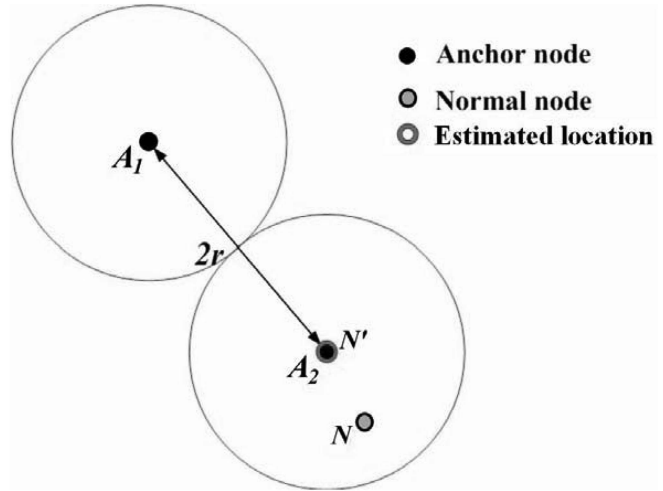


Fig. 4. Relative locations of the near anchor and the farther anchor.

between  $A_2$  and  $A_1$  (or  $A_3$ ) is less than  $2r$ , by using two-hop flooding, the near anchor  $A_2$  can gather the ID and location information from the farther anchors  $A_1$  and  $A_3$ . Since the distance between anchor  $A_4$  and anchor  $A_2$  is more than  $2r$ , and anchor  $A_4$  is too far to affect the estimated location of the normal node  $N_1$ , anchor  $A_2$  will not be able to gather the ID and location information of anchor  $A_4$ . After each anchor has collected the location information of anchors within two hops, each anchor will broadcast the collected location information to normal nodes within one hop. The normal node  $N_1$  will then receive the beacon from its near anchor  $A_2$ . Finally, every node will have the ID and the location information of both near and farther anchors.

### 3.2 Improved Grid-Scan Algorithm

After finishing the first phase, each normal node can use the connectivity constraints collected from both near and farther anchors to estimate its location. The connectivity constraints can be further categorized as either "positive connectivity constraints" or "negative connectivity constraints." If a normal node is within the communication range of the anchors, we can say that there are positive connectivity constraints between the normal node and the near anchors. Fig. 6 shows examples of positive connectivity constraints. When a normal node receives a beacon from a near anchor, the normal node comes within the communication range of the anchor. Additionally, when a normal

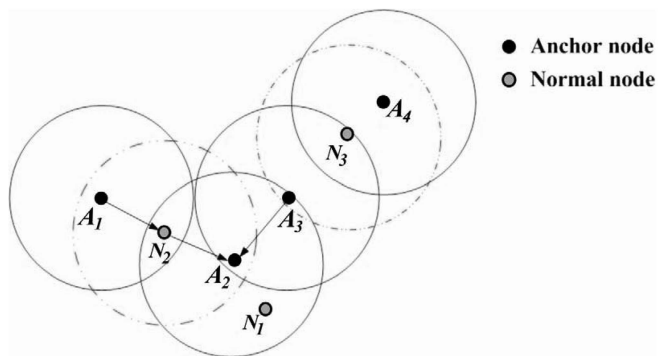


Fig. 5. Beacon exchange via two-hop flooding.

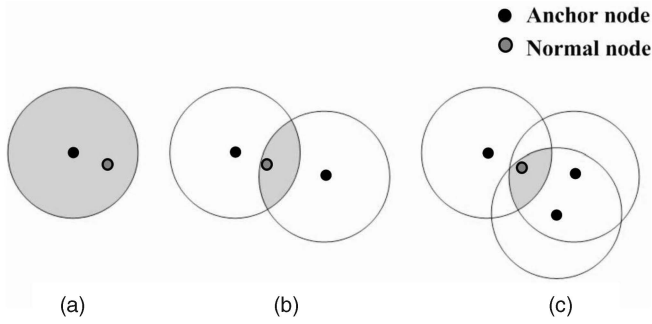


Fig. 6. Examples of positive connectivity constraints.

node receives beacons from several anchors, the normal node is within the intersection of these near anchors' communication regions. Therefore, the normal nodes can estimate their own location according to the positive connectivity constraints of near anchors. In Fig. 6, the shaded region is the region where the normal node may reside, and we call the shaded region the "estimative region." Increasing positive connectivity constraints may lead to a smaller estimative region, as shown in Fig. 6c.

For the ease of estimation, we use a square that bounds the communication region of the anchor to represent the communication region of the anchor, as shown in Fig. 7a. The ER of the normal node is defined as the intersection of those squares that bound the communication regions of anchors. The four sides of the ER are either parallel with the  $x$ -axis or with the  $y$ -axis. Fig. 7 shows the ER of the estimative regions in Fig. 6. The definition of our ER is different from that of the CPE algorithm's [14] and is easier to compute. In some cases, since our ER may not totally fit the estimative region, it is not rational to regard the center of our ER as the initial estimated location of the normal node.

Thus, we use an improved grid-scan algorithm to calculate the initial estimated location of the normal node. The grid-scan algorithm has been previously used by APIT [13], which is also a range-free localization scheme. Unlike the grid-scan algorithm, which scans each grid in the whole network area, the improved grid-scan algorithm merely scans each grid in the ER. We use the improved grid-scan algorithm to calculate the estimative region and regard the center of the estimative region as the initial estimated location of the normal node. The detail of the algorithm is described in the following paragraphs.

For the ease of explaining the improved grid-scan algorithm, we define some notations below. Assume that the length of the ER is equal to  $L \times S$ , the width of the ER

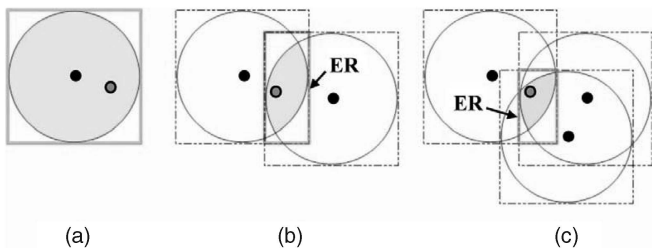


Fig. 7. Examples of ERs.

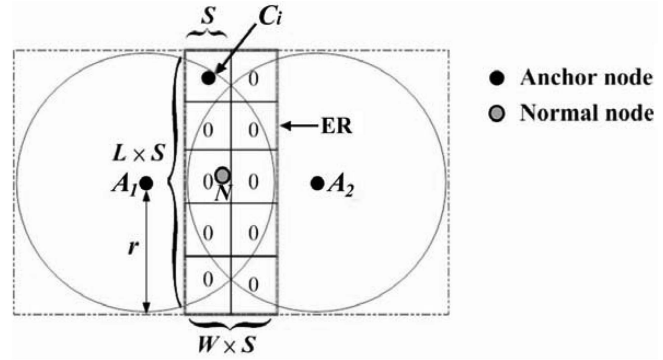


Fig. 8. Examples of the notations.

is equal to  $W \times S$ , and the edge length of the grids is equal to  $S$ , as shown in Fig. 8. The ER of the normal node is divided into a set of grids  $G = \{G_1, G_2, \dots, G_n\}$ , where  $n$  is equal to  $L \times W$ . Each grid is assigned an initial value 0.  $C_i$  represents the center of the grid  $G_i$ . If  $C_i$  is within the communication range of  $m$  near anchors, the value of the grid  $G_i$  increases by  $m$ . Therefore, the grid value indicates the number of anchors whose communication region covers the center of the grid. Once all grid values are computed, the grids with the greatest grid values are the regions where the normal node may reside.

Figs. 9 and 10 are examples that show how the improved grid-scan algorithm works. First, as shown in Fig. 9, the ER of normal node  $N$  is calculated. Then, the ER is divided into smaller grids, and the initial value of each grid is set to 0. Finally, by judging whether each grid overlaps with the communication region of each near anchors  $A_1, A_2$ , and  $A_3$ , the final value of each grid is obtained. In Fig. 10, the grid with the greatest grid value (3) is the grid whose center is covered by the communication regions of all the three near anchors. These grids form a region where node  $N$  may reside.

Assume that there are  $k$  grids with the greatest grid value. The coordinate of the initial estimated location can be derived from the coordinates of the  $k$  grids' center. By summing up the  $x$ -coordinates of the centers of the  $k$  grids and dividing the sum by  $k$ , we can derive the  $x$ -coordinate of the initial estimated location. Using this same method, we can also derive the  $y$ -coordinate of the initial estimated location. In Fig. 10,  $N'$  is the initial estimated location of the normal node  $N$ . Reducing the size of the grid may reduce location errors caused by granularity. However, it increases the calculation load. In our simulation, the grid size is set to

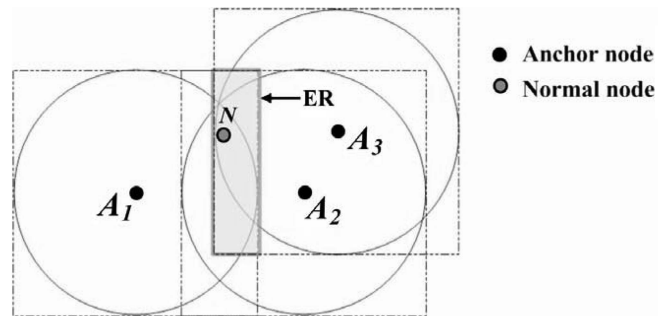


Fig. 9. The ER of the normal node  $N$ .

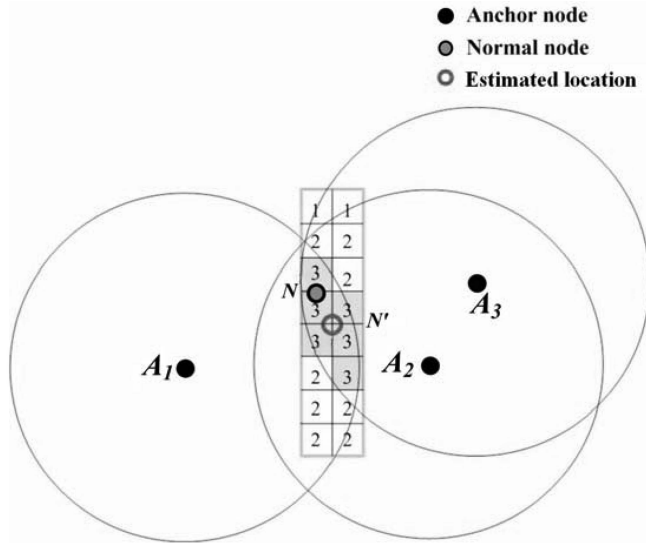


Fig. 10. Initial estimated location.

$0.1r \times 0.1r$  so as to guarantee the estimative accuracy and so that it would not cost too much computation time.

### 3.3 Refinement

The initial estimated location derived by the improved grid-scan algorithm can be further refined according to “negative connectivity constraints.” If a normal node can acquire the locations of farther anchors through its neighbors, we can say that there are negative connectivity constraints between the normal node and the farther anchors. The initial estimated location of the normal node can be refined according to the relative location of the farther anchors and the intersection of the near anchors’ communication regions.

#### 3.3.1 The Impact of the Farther Anchor

Figs. 11 and 12 show the impact of the farther anchors. The more the farther anchor’s communication region overlaps with the intersection of the near anchor’s communication region, the more refinement will be obtained for the initial estimated location. In Fig. 11, anchors  $A_2$  and  $A_1$  are the near and farther anchors, respectively, of the normal node  $N$ . According to the positive connectivity constraint mentioned in Section 3.2, the normal node  $N$  will calculate its ER and then use the improved grid-scan algorithm to obtain its initial estimated location  $N'$ , which is equal to the only near anchor  $A_2$ .

We use the concept of repulsive virtual force (VF) to represent the impact made by each farther anchor on the initial estimated location of the normal node. The intensity of the VF is proportional to how much the communication region of a farther anchor overlaps with the intersection of the near anchors’ communication regions. Here is an example to explain it. In Fig. 12, the line  $L_1$  is the straight line that passes through the farther anchor  $A_1$  and the initial estimated location  $N'$ . We define  $D_{invasion_{A_1}}$  (the invasion distance of farther anchor  $A_1$ ) as the segment of line  $L_1$  within the intersection of the farther anchor’s communication region and the intersection of the near anchors’ communication regions. The more the communication

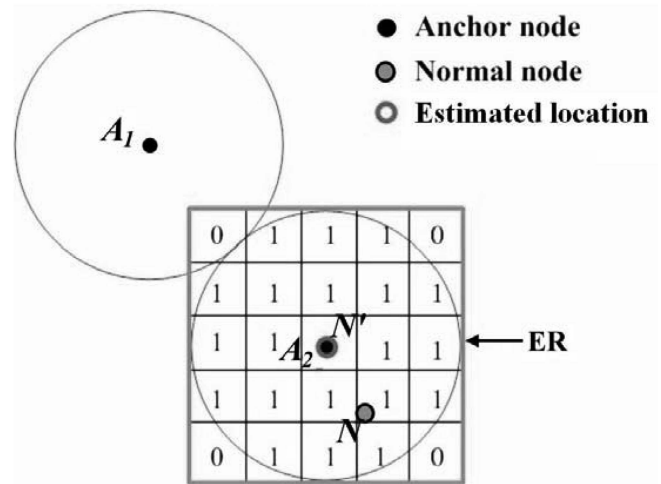


Fig. 11. Initial estimated location.

region of the farther anchor overlaps with the near anchors’ communication region, the longer  $D_{invasion_{A_1}}$  becomes. Thus, the intensity of the VF is proportional to the length of  $D_{invasion_{A_1}}$ . The direction of the VF is from the farther anchor  $A_1$  toward the initial estimated location  $N'$ .

In Fig. 11, the normal node  $N$  has only one near anchor  $A_2$ , and there is no intersection between the near anchor  $A_2$  and the farther anchor  $A_1$ ’s communication region. Thus, the intensity of the VF caused by the farther anchor  $A_1$  is zero, and the initial estimated location  $N'$  does not need to be corrected. In Fig. 12, there is an intersection between the communication regions of the farther anchor  $A_1$  and the near anchor  $A_2$ . It is obvious that the farther anchor  $A_1$  invades the communication region of the near anchor  $A_2$  and causes the VF to push the initial estimated location toward the lower right. As shown in Fig. 12, the stronger the VF is, the greater  $D_{invasion_{A_1}}$  becomes. In Fig. 12, the refined estimated location  $N''$  is much closer to the real location of the normal node  $N$ . How to derive the VF is described in Section 3.3.2.

#### 3.3.2 Refinement of the Estimated Location

The refinement phase runs concurrently at each normal node. In Fig. 13, node  $N$  is a normal node, node  $A_1$  is the

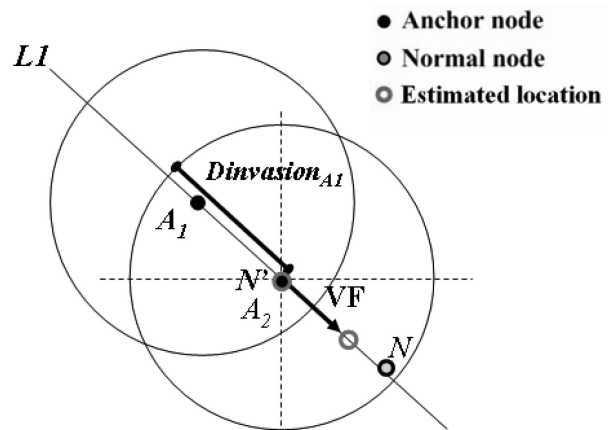
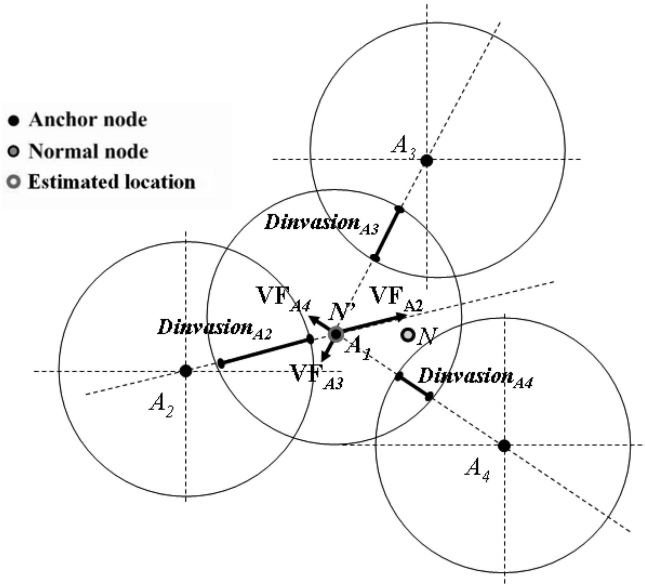


Fig. 12. The VF is proportional to the  $D_{invasion_{A_1}}$ .

Fig. 13. Relation between  $VF_{A4}$  and  $Divasion_{A4}$ .

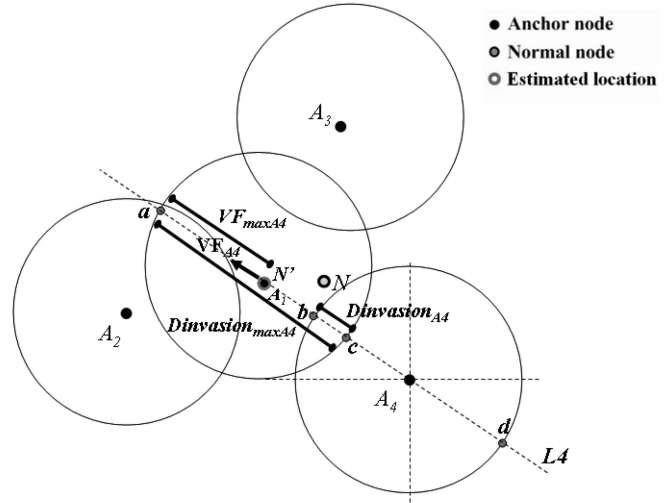
near anchor of node  $N$ , and nodes  $A_2$ ,  $A_3$ , and  $A_4$  are the farther anchors of node  $N$ . In this example, there is only one positive connectivity constraint, so the location of the near anchor  $A_1$  is also the initial estimated location  $N'$  of the normal node  $N$ . The VF caused by the farther anchor  $A_2$  is denoted as  $VF_{A2}$ , and the direction of  $VF_{A2}$  is from the farther anchor  $A_2$  toward the initial estimated location  $N'$ .  $VF_{A2}$  will push  $N'$  toward the upper right. Similarly,  $VF_{A3}$  and  $VF_{A4}$  will push  $N'$  toward the lower left and upper left, respectively. The intensity of  $VF_{A2}$ ,  $VF_{A3}$ , and  $VF_{A4}$  is proportional to the length of each  $Divasion$ . Finally, the initial estimated location  $N'$  of the normal node  $N$  is pushed according to the intensity and direction of the resultant virtual forces (RVFs). We derive the relation between the intensity of VF and the length of  $Divasion$  by observing the following example.

In Fig. 14,  $Divasion_{A4max}$  is the maximum possible invasion distance of the farther anchor  $A_4$  toward the near anchor  $A_1$ . When there is only one near anchor,  $Divasion_{A4max}$  is equal to the diameter ( $\overline{ac}$ ) of near anchor  $A_1$ 's communication region. When  $Divasion_{A4} = Divasion_{A4max} = \overline{ac}$ , we need to push  $N'$  from the center to the boundary of  $A_1$ 's communication region, so we have  $|VF_{A4}| = |VF_{A4max}| = |\overline{N'a}|$ . Since the intensity of VF is proportional to the length of  $Divasion$ , we can derive the intensity of  $VF_{A4}$  (denoted  $|VF_{A4}|$ ) with the following equation:

$$|VF_{A4}| = |Divasion_{A4}| \times \frac{|VF_{A4max}|}{|Divasion_{A4max}|}.$$

Let  $V_{A4}$  be the unit vector in the direction from the farther anchor  $A_4$  toward the initial estimated location  $N'$ .  $V_{A4}$  can be derived with the following equation:

$$V_{A4} = \frac{\overrightarrow{Divasion_{A4}}}{|Divasion_{A4}|}, \quad \text{where } \overrightarrow{Divasion_{A4}} \text{ is vector } \overline{cb}.$$

Fig. 14. Relation between VF and  $Divasion$ .

Assume that the vector to represent  $VF_{A4}$  is denoted as  $\overrightarrow{VF_{A4}}$ . We can derive  $\overrightarrow{VF_{A4}}$  with the following equation:

$$\begin{aligned} \overrightarrow{VF_{A4}} &= V_{A4} \times |VF_{A4}| \\ &= \frac{\overrightarrow{Divasion_{A4}}}{|Divasion_{A4}|} \times |Divasion_{A4}| \times \frac{|VF_{A4max}|}{|Divasion_{A4max}|} \\ &= \overrightarrow{Divasion_{A4}} \times \frac{|VF_{A4max}|}{|Divasion_{A4max}|}. \end{aligned}$$

Assume that the line passes through the farther anchor  $A_i$  and the initial estimated location  $N'$  is denoted as  $L_i$ , the segment of line  $L_i$  within the intersection of the farther anchor's communication region and the intersection of the near anchors' communication regions is denoted as  $Divasion_{Ai}$ , the maximum possible invasion distance of the farther anchor  $A_i$  is denoted as  $Divasion_{Aimax}$ , the corresponding VF is denoted as  $VF_{Aimax}$ , and the vector to represent  $VF_{Ai}$  is denoted as  $\overrightarrow{VF_{Ai}}$ . To derive  $\overrightarrow{VF_{Ai}}$ , we need to calculate the coordinates of the two end points of  $Divasion_{Aimax}$  and  $Divasion_{Ai}$ . To derive the coordinates of the two end points of  $Divasion_{Aimax}$ , the normal node  $N$  computes the coordinates of the two intersection points of line  $L_i$  and the boundary of the estimative region. The two intersection points of line  $L_i$  and the boundary of the near anchors' communication regions that are closest to  $N'$  are the two end points of  $Divasion_{Aimax}$  (e.g., points  $a$  and  $c$  in Fig. 14). Between the two end points of  $Divasion_{Aimax}$ , the end point that is closer to the farther anchor  $A_i$  is regarded as the end point of both  $Divasion_{Aimax}$  and  $Divasion_{Ai}$  (e.g., point  $c$  in Fig. 14). To derive the coordinate of the other end point of  $Divasion_{Ai}$ , the normal node  $N$  computes the coordinates of the intersection points of line  $L_i$  and the boundary of the communication regions of the farther anchor  $A_i$ . The intersection point of line  $L_i$  and the boundary of the farther anchor  $A_i$ 's communication region between  $N'$  and one of the end points of  $Divasion_{Aimax}$  (e.g., point  $c$  in Fig. 14) is regarded as the other end point of  $Divasion_{Ai}$  (e.g., point  $b$  in Fig. 14).

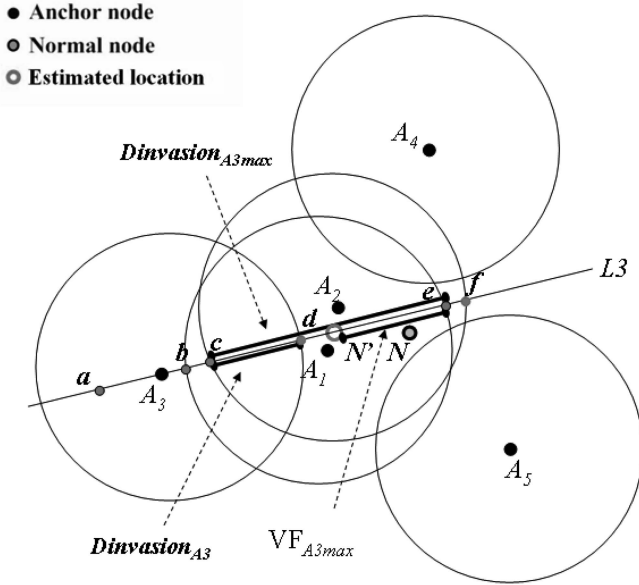


Fig. 15. Example of two near anchors and three farther anchors.

For example, in Fig. 15, the intersection points of line  $L_3$  and the boundary of the communication regions of near anchors  $A_1$  and  $A_2$  are  $b$ ,  $c$ ,  $e$ , and  $f$ . Among points  $b$ ,  $c$ ,  $e$ , and  $f$ , points  $c$  and  $e$  are closest to  $N'$ , so they are regarded as the two end points of  $Dinvasion_{A3max}$ . Between points  $c$  and  $e$ , point  $c$  is closer to the farther anchor  $A_3$ , so it is regarded as the end point of both  $Dinvasion_{A3max}$  and  $Dinvasion_{A3}$ . The intersection points of line  $L_3$  and the boundary of the communication regions of the farther anchor  $A_3$  are  $a$  and  $d$ . Point  $d$  is between  $N'$  and point  $c$ , so it is regarded as the other end point of  $Dinvasion_{A3}$ .

Therefore, we have  $\overrightarrow{Dinvasion_{A3}} = \overrightarrow{cd}$ ,  $Dinvasion_{A3max} = \overline{ce}$ , and  $VF_{A3max} = \overline{N'e}$ . Assume that the coordinates of points  $c$ ,  $d$ ,  $e$ , and  $N'$  are denoted as  $(x_c, y_c)$ ,  $(x_d, y_d)$ ,  $(x_e, y_e)$ , and  $(x_{n'}, y_{n'})$ , respectively. We have  $\overrightarrow{cd} = (x_d - x_c, y_d - y_c)$ ,  $|Dinvasion_{A3max}| = \sqrt{(x_e - x_c)^2 + (y_e - y_c)^2}$ ,  $|VF_{A3max}| = \sqrt{(x_e - x_{n'})^2 + (y_e - y_{n'})^2}$ , and in a similar manner, we can derive  $\overrightarrow{VF_{A4}}$  and  $\overrightarrow{VF_{A5}}$ . By summing up  $\overrightarrow{VF_{A3}}$ ,  $\overrightarrow{VF_{A4}}$ , and  $\overrightarrow{VF_{A5}} = \overrightarrow{cd} \times \frac{|VF_{A3max}|}{|Dinvasion_{A3max}|} = (x_d - x_c, y_d - y_c) \times \frac{\sqrt{(x_e - x_{n'})^2 + (y_e - y_{n'})^2}}{\sqrt{(x_e - x_c)^2 + (y_e - y_c)^2}}$ .  $\overrightarrow{VF_{A5}}$ , we can derive  $RFV$ .

After a normal node has calculated its own estimated location through the above three phases, it will broadcast its own estimated location, as well as the location information collected before to its one-hop neighbors. Thus, a normal node, which does not have any neighboring anchors, will regard these neighboring normal nodes as anchors and use location information collected from these normal nodes to estimate its own location. When a new node joins the network, it will send a beacon packet to request location information from its one-hop neighbors. After collecting the location information from its one-hop neighbors, the new node can then estimate its own location. The pseudocode of our DRLS is shown as follows:

#### Distributed Range-Free Localization Scheme:

**For each anchor node:** Gather the ID and locations of anchors within two hops via two-hop flooding and then broadcast the collected anchors' locations to normal nodes within one hop.

**For each normal node:** Use the improved grid-scan algorithm to calculate the initial estimated location using the following steps:

1) Divide the  $ER$  into a set of grids.

2) **For each grid within ER do**

Calculate the number (denoted as  $m$ ) of near anchors whose communication region covers the center of the grid and increases the grid value by  $m$ .

**End for**

3) Let  $x_{n'} = \sum_{i=1}^k x_i/k$  and  $y_{n'} = \sum_{i=1}^k y_i/k$ , where  $(x_{n'}, y_{n'})$  is the coordinate of the initial estimated location  $N'$ ,  $(x_i, y_i)$  are the coordinates of the  $i$ th grid with the greatest grid value, and  $k$  is the number of grids with the greatest grid value.

**If** there exists at least one farther anchor node overlapping with the intersection of the near anchors' communication regions **then** /\* Refinement Scheme \*/

Correct the initial estimated location using the following steps:

**For each farther anchor  $A_i$  do**

1) Calculate the coordinates of the two end points of  $Dinvasion_{imax}$  (denoted as  $a_i$  and  $c_i$ ) and  $Dinvasion_i$  (denoted as  $b_i$  and  $d_i$ ).

2) Let  $\overrightarrow{VF_i} = Dinvasion_i \times |VF_{imax}| / |Dinvasion_{imax}| = \overrightarrow{cb} \times |\overline{ac}| / |\overline{N'a}|$ .

**End for**

Let  $RFV = \sum_{i=1}^n \overrightarrow{VF_i}$ , where  $n$  is the number of farther anchors.

Correct the initial estimated location by adding  $RFV$  to the initial estimated location.

**End if**

Broadcast the estimated location information to its neighbors.

## 4 PERFORMANCE EVALUATION

In this section, we compare the performance of the proposed DRLS with that of the existing range-free localization schemes mentioned in Section 2.2, including the Centroid method [8] and the CPE localization scheme [14]. We do not compare them with the APIT and DLE because the sensor nodes are not homogeneous in APIT and DLE, which means that the communication range of the anchor is larger than that of the normal node. However, in our DRLS, all sensor nodes are homogeneous and have the same fixed communication range  $r$ , where  $r$  is the communication range of the sensor nodes. In DRLS, nodes and anchors are randomly distributed in a  $10r \times 10r$  square region. Each node has a unique ID, and the size of the grid is  $0.1r \times 0.1r$  to guarantee the estimative accuracy and so that it would not cost too much calculation time and memory. We do not discuss collision problems in the simulations because we assume that they can be solved by the MAC layer protocols.

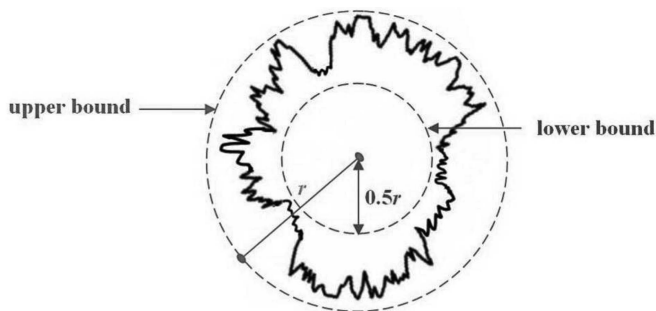


Fig. 16. Radio propagation pattern.

#### 4.1 Simulation Parameter

We use NS2 as the simulator. In the simulation, we vary two parameters, the anchor ratio and the radio propagation patterns. The anchor ratio is defined as  $m/(n+m)$ , where  $n$  is the number of normal nodes, and  $m$  is the number of anchors in the WSN. We vary the radio propagation pattern in the simulation because the assumption of a circular communication range is not realistic in the real world. The problems of multipath fading, unstable signal propagation, and background noise make the communication radius of the sensor node unfixed. To verify that the DRLS is usable in the real world, we use the radio model proposed in [13]. In this model, the communication radius of the sensor node is irregular, and the notation DOI is used to represent the degree of irregularity. There are the upper bound and the lower bound of the communication radius. The upper bound is the ideal communication radius  $r$ , and the lower bound is proportional to  $(1 - DOI)$ . For example, if the upper bound is  $r$  and the DOI is 0.5, then the lower bound is  $(1 - DOI) = 0.5r$ . If a sensor node is outside the upper bound of the communication radius of another sensor node, it will not receive the beacon packets from that sensor node. On the other hand, if a sensor node is inside the lower bound of the communication radius of another sensor node, it can always receive the beacon packets from that sensor node. The radio range in any direction varies randomly between the upper bound and the lower bound. The radio pattern is shown in Fig. 16.

In the following, we compare the mean error and the communication costs among each of the localization schemes through simulations and real experiments. We also analyze the computation costs among each of the localization schemes. The localization error is the distance between the estimated location and the physical location of the normal node, and the mean error can be calculated as the average localization error of all normal nodes.

Fig. 17 shows the impact of simulation times on the size of the confidence interval. As the simulation times increase, the size of the confidence interval becomes smaller. Similarly, as the number of sensor nodes increases, the size of the confidence interval becomes smaller. We have observed that the size of the confidence interval gradually converges when the simulation times approach 100. Therefore, we obtain the simulation results from 100 times of simulations for each set of parameters. In the worst case, the ratio of the size of the 95 percent confidence interval to the

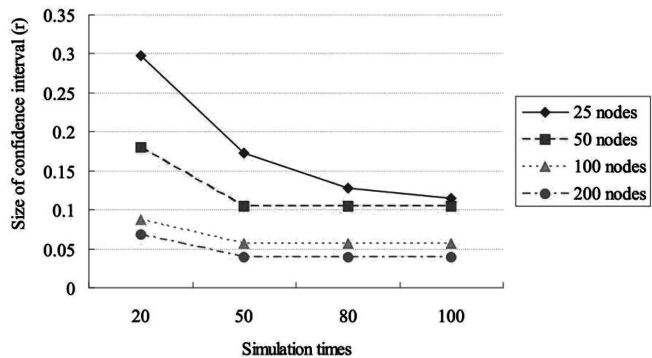


Fig. 17. Simulation times versus the size of the confidence interval (Anchor ratio = 40 percent, DOI = 0.7).

mean value is less than 0.04, which should be able to give statistical meaning to collected data.

#### 4.2 Effect of Varying Anchor Ratio

In this section, we vary the anchor ratio to see its impact on the mean error. The area size of the WSN is  $10r \times 10r$ . The total number of sensor nodes is 200. We vary the number of anchors from 10 to 95. Fig. 18 shows the impact of the anchor's ratio on the mean error. As the number of anchors increases, the mean error decreases. More near anchors may bring more positive connectivity constraints to reduce the size of the estimative region and, thus, increase the accuracy of the initial estimated location. The farther anchors may bring even more negative connectivity constraints to refine the initial estimated location and, thus, increase the accuracy of the estimated location. The decreasing curve tends to become smooth when the number of total anchors is over 70. When the ratio of the anchors goes over a certain degree, the size of the estimative region cannot be greatly reduced, and thus, the impact becomes smaller. DRLS performs better in terms of accuracy because the Centroid and CPE only utilize the positive connectivity constraints to acquire the estimated location.

In Fig. 19, we demonstrate the mean error range of the DRLS and other localization schemes. The mean error range is proportional to the difference between the maximum mean error and the minimum mean error. The DRLS is more stable compared to other localization schemes because its mean error range is much smaller than the others.

#### 4.3 Communication Costs

In this section, we vary the anchor ratio to see its impact on communication costs. The results can be found in Fig. 20. As the ratio of anchors increases, communication costs also increase. The communication costs of the Centroid scheme are the lowest because it only collects one hop information, while the DRLS collects both positive and negative connectivity constraints by two-hop flooding. Therefore, the communication costs of the DRLS scheme are higher than that of the Centroid scheme. However, with both positive and negative connectivity constraints, the DRLS scheme can acquire more accurate estimated location. Thus, there is a trade-off between the localization accuracy and the communication costs. The communication costs of the CPE scheme are much higher than those of the other localization schemes because the CPE is a centralized localization scheme. The normal nodes need to send

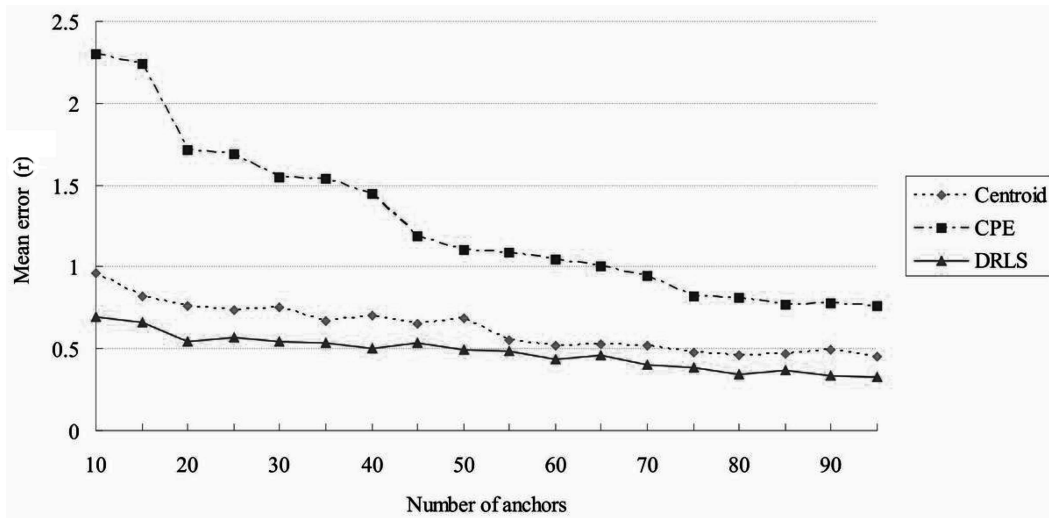


Fig. 18. Anchor ratio versus mean error (number of sensor nodes = 200).

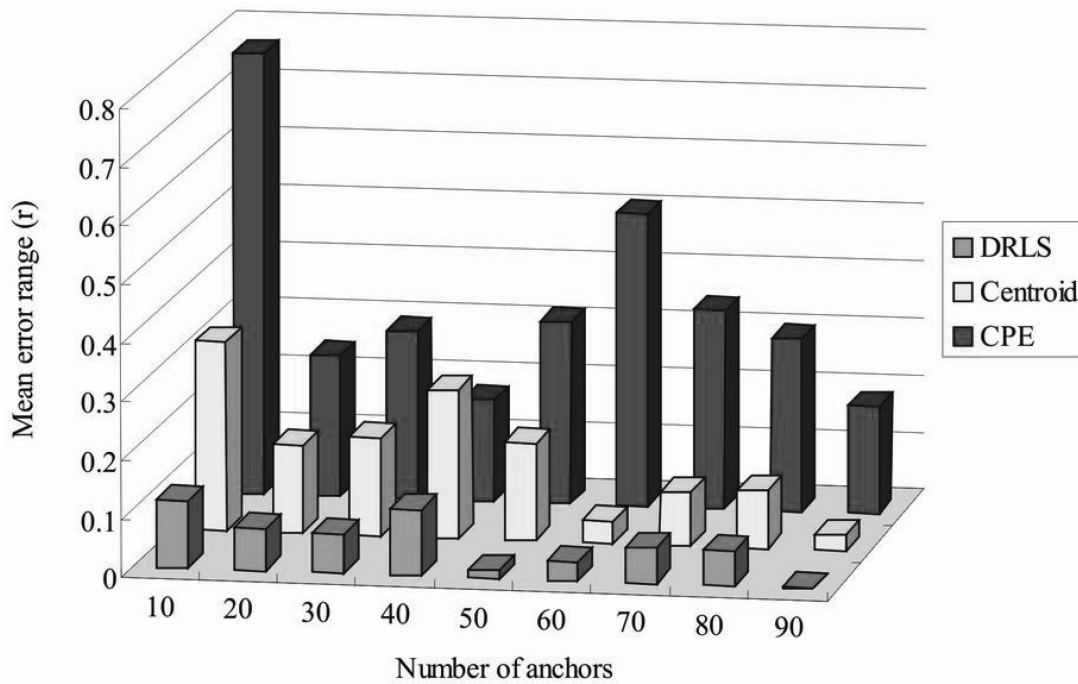


Fig. 19. Anchor ratio versus mean error range.

location information back to the central controller, which will calculate the estimated location of each normal node and then send back to each normal node.

#### 4.4 Effect of Varying Density of Nodes

In this section, we fix the ratio of anchors and vary the number of sensor nodes to see the impact of a node's density on the mean error. The area size is fixed ( $10r \times 10r$ ). The ratio of anchors is set at 40 percent. The number of sensor nodes varies from 50 to 250. In Fig. 21, we can see that the mean error decreases as the number of nodes increases. In addition, the DRLS performs better than other localization schemes.

#### 4.5 Effect of Irregular Communication Radius

In this simulation, we demonstrate the impact of irregular communication radius on the mean error of the DRLS and other localization schemes. The total number of sensor

nodes is fixed at 200. In Fig. 22, the ratio of anchors is tuned between 7.5 percent and 47.5 percent. As the DOI increases, the possibility that a normal node cannot hear beacon packets from near anchors or farther anchors increases, and thus, the mean error also increases. As shown in Fig. 22, we can see how DOI affects the mean error of each localization scheme. The mean error of DRLS increases as the DOI increases because the normal node will receive less beacon packets from both near anchors and farther anchors. However, the mean error of the DRLS is still lower than that of other localization schemes because of the refinement scheme. Thus, the DRLS is more robust than other schemes. The reason why the mean error of Centroid and CPE increases with DOI is that the normal node receives less beacon packets from near anchors. As shown in Fig. 22, as the ratio of anchors increases, the possibility that a normal node will receive the beacon packets from near anchors or

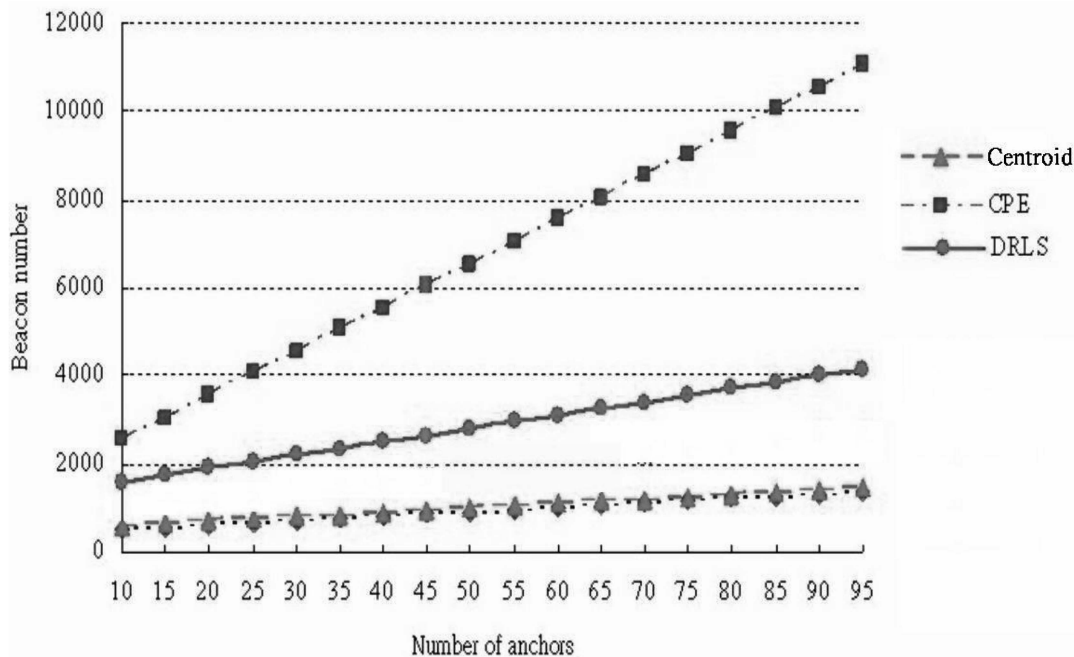


Fig. 20. Ratio of anchors versus communication overhead.

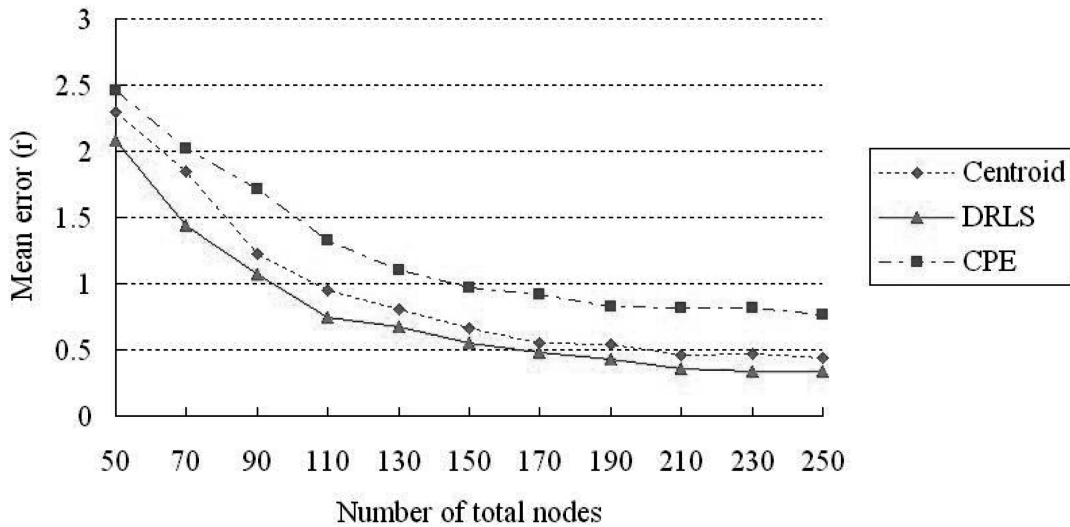


Fig. 21. Density of nodes versus mean error (Ratio of anchors = 40 percent).

farther anchors also increases and, thus, improves the accuracy of the estimated location. When the ratio of anchors is low, the DRLS scheme performs much better than the other two schemes in terms of accuracy, which indicates that the DRLS scheme can achieve the same accuracy as the Centroid and CPE schemes with a lower ratio of anchors, thus reducing the hardware cost.

#### 4.6 Analysis of Computation Costs

The computation cost of Centroid is the lowest because each normal node only needs to compute the average coordinates of the neighboring anchors. The total computation cost of the Centroid scheme is  $n$ , where  $n$  is the total number of normal nodes. As for the computation cost of CPE and DRLS, both CPE and DRLS need to calculate the ER. However, CPE needs to calculate the exact rectangle that bounds the intersection of the communication regions, while DRLS only needs to calculate the intersection of the

rectangles that bound the communication regions of neighboring anchors. Therefore, it is easier to compute the ER of DRLS than that of CPE. Assume that the average number of each normal node's neighboring anchors is  $k$ . Then, there are  $C(k, 2) = k(k-1)/2$  pairs of anchors to form  $k(k-1)/2$  ERs for each normal node to calculate the intersection of the  $k(k-1)/2$  ERs. Hence, the total computation cost of CPE is  $nk(k-1)/2$ . However, to derive the ER of DRLS, each normal node only needs to calculate the intersection of the  $k$  rectangles that bound each of the communication regions of the  $k$  anchors. Hence, the total computation cost to calculate the ER of the DRLS is  $nk$ . After the ER is computed, the DRLS needs to scan grids in the ER and calculate the resultant of the VFs. Because the area size of the ER is no greater than  $4r^2$  and the grid size is  $0.1r \times 0.1r$ , the number of grid is no more than 400, and the computation cost of grid scan is no more than  $400k$ , where  $r$

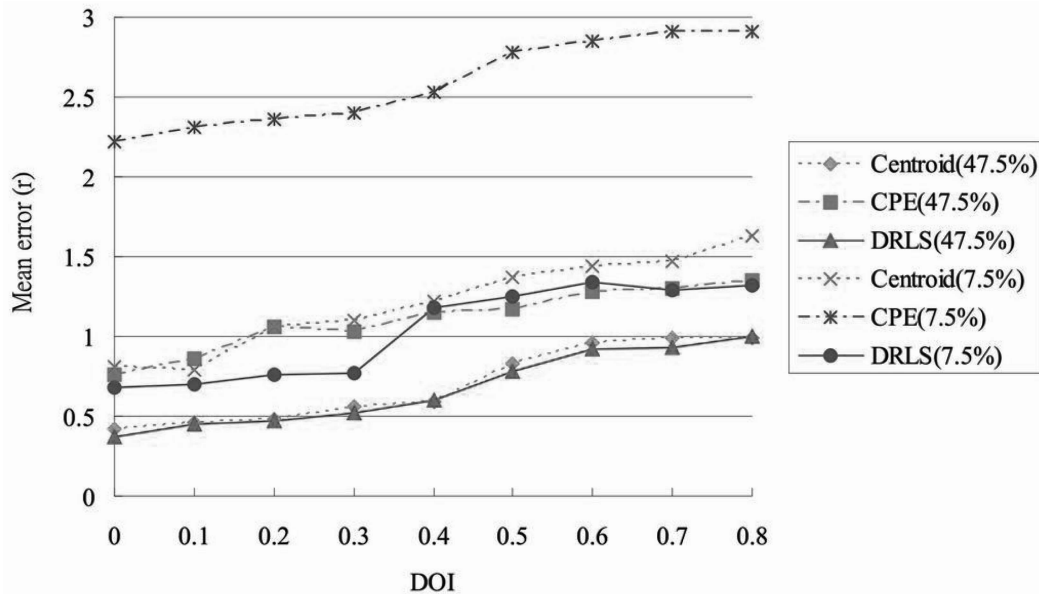


Fig. 22. DOI versus mean error (anchor ratio = 7.5 percent ~ 47.5 percent).

is the communication radius. Hence, each node's computation cost of grid scan can be considered as  $Ck$ , where  $C$  is the number of grids. As for the calculation of the resultant of the VFs, each node's computation cost is  $m$ , where  $m$  is the average number of farther anchors. The total computation cost of the DRLS scheme is  $n((C + 1)k + m)$ .

#### 4.7 Experimental Results

To demonstrate the accuracy of the proposed scheme, we have implemented the CPE, Centroid, and the proposed scheme in a real WSN, which is formed by 15-25 Octopus I sensor nodes, as shown in Fig. 23. The Octopus I is an IEEE 802.15.4-compliant wireless sensor node, which is composed of an AVR Atmega128 microcontroller and a Chipcon CC2420 module. The Chipcon CC2420 supports 32 power levels setting for data transmission. According to our experiments, the maximum transmission range is able to reach 80 m, and the minimum transmission range is around 20 cm in an open environment. For the ease of measuring the location of each sensor node and collecting the estimated results, in the following experiments, we use the minimum transmission power level for data transmission and assume that the communication radius of each sensor node is 20 cm. Although the testbed is an obstacle-free environment, we believe that it can still reflect the effects of irregular communication radius and unreliable transmissions. The network size is 150 cm  $\times$  105 cm, the radio frequency is 2.4 GHz, and the RF power is  $-25$  dBm. The experiments are done by tuning two parameters: the density of sensor nodes and the ratio of anchors. Each result is derived from 20 experiments.

##### 4.7.1 Impact of Node's Density

To see the impact of node's density on mean error, the total number of sensor nodes is tuned between 15 and 25. The ratio of anchors is fixed at 33 percent. Fig. 24 shows the impact of node's density on mean error. Similar to the simulation results, as the number of sensor node increases,

the mean error decreases. As the node density increases, more location information can be collected, thus improving the accuracy of the estimated location. The DRLS scheme still outperforms the other schemes because it uses both positive and negative connectivity constrains to refine the estimated locations.

##### 4.7.2 Impact of the Ratio of Anchors

To see the impact of anchor's ratio on mean error, the ratio of anchors is tuned between 20 percent and 33 percent. The total number of sensor nodes is fixed at 25. Fig. 25 shows the impact of anchor's ratio on mean error. Similar to the simulation results, as the ratio of anchors increases, the mean error decreases. As the ratio of anchors increases, more connectivity constraints can be collected, thus improving the accuracy of the estimated location. The DRLS scheme still outperforms the other schemes because it uses both neighboring and farther anchors' location information to refine the estimated locations.

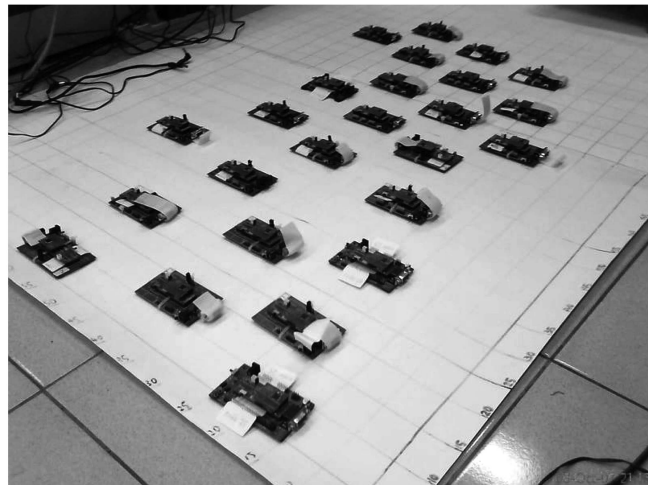


Fig. 23. The testbed of our experiments.

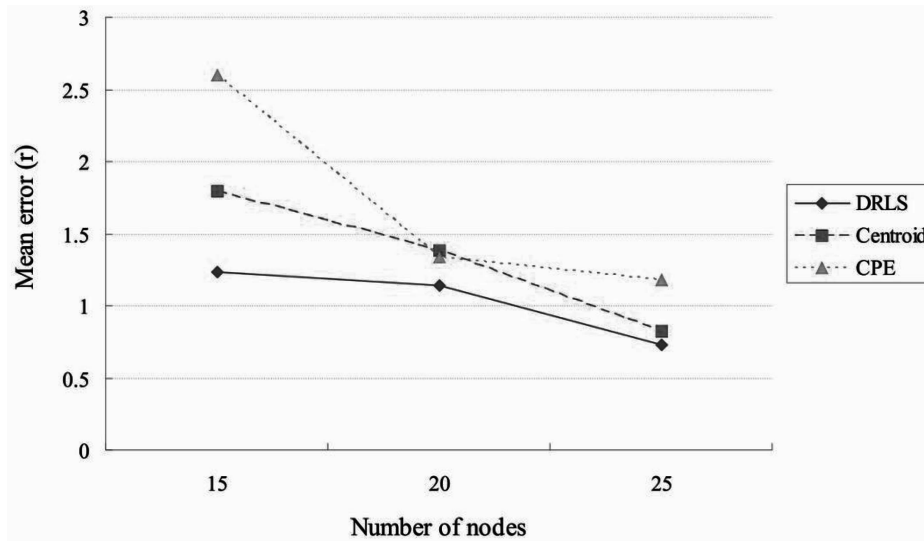


Fig. 24. Node's density versus mean error (ratio of anchors = 33 percent).

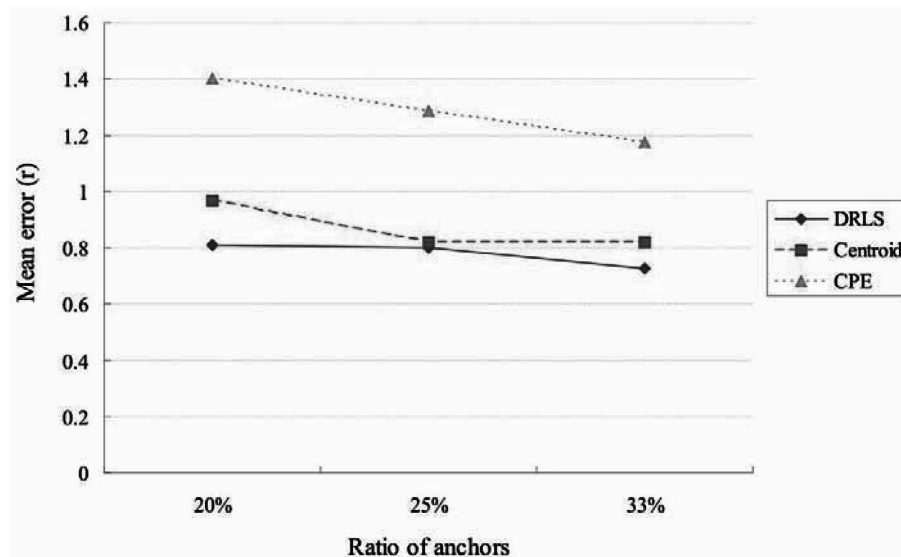


Fig. 25. Anchor's ratio versus mean error (number of sensor nodes = 25).

## 5 CONCLUSIONS

Localization is a fundamental and essential issue for WSNs. To reduce the communication and computation cost and improve the accuracy of the estimated location, we have proposed a fully distributed range-free localization scheme for WSNs. In the proposed scheme, each normal node gathers the necessary information via two-hop flooding and is thus scalable. Aside from this, each normal node uses a simplified approach to calculate the ER and the proposed improved grid-scan algorithm to find the initial estimated locations of the normal node, thus reducing the computation cost. Furthermore, we have proposed a vector-based refinement scheme to correct the initial estimated location of the normal node, thus improving the accuracy of the estimated location. Analysis, simulation, and experimental results have shown that the proposed scheme can achieve better accuracy than the other localization schemes with reasonable communication and computation costs, even when the communication radius is irregular.

## ACKNOWLEDGMENTS

This work was supported by the National Science Council of Taiwan, R.O.C., under Grant NSC 95-2221-E-008-018 and Grant NSC-96-2752-E-007-003-PAE.

## REFERENCES

- [1] A. Savvides, C.-C. Han, and M.B. Strivastava, "Dynamic Fine-Grained Localization in Ad-Hoc Networks of Sensors," *Proc. ACM MobiCom '01*, pp. 166-179, July 2001.
- [2] N.B. Priyantha, A. Chakraborty, and H. Balakrishnan, "The Cricket Location-Support System," *Proc. ACM MobiCom '00*, pp. 32-43, Aug. 2000.
- [3] A. Nasipuri and K. Li, "A Directionality Based Location Discovery Scheme for Wireless Sensor Networks," *Proc. Int'l Conf. Wireless Sensor Networks and Applications*, pp. 105-111, Sept. 2002.
- [4] M.M. Patil, U. Shaha, U.B. Desai, and S.N. Merchant, "Localization in Wireless Sensor Networks Using Three Masters," *Proc. Int'l Conf. Personal Wireless Comm.*, pp. 384-388, Jan. 2005.
- [5] Y. Ohta, M. Sugano, and M. Murata, "Autonomous Localization Method in Wireless Sensor Networks," *Proc. Int'l Workshop Sensor Networks and Systems for Pervasive Computing*, pp. 379-384, Mar. 2005.

- [6] N.B. Priyantha, H. Balakrishnan, E. Demaine, and S. Teller, "Anchor-Free Distributed Localization in Sensor Networks," *Proc. ACM Int'l Conf. Embedded Networked Sensor Systems (SenSys '03)*, pp. 340-341, Nov. 2003.
- [7] J. Albowicz, A. Chen, and L. Zhang, "Recursive Position Estimation in Sensor Networks," *Proc. Int'l Conf. Network Protocols*, pp. 35-41, Nov. 2001.
- [8] N. Bulusu, J. Heidemann, and D. Estrin, "GPS-Less Low Cost Outdoor Localization for Very Small Devices," *IEEE Personal Comm. Magazine*, vol. 7, no. 5, pp. 28-34, Oct. 2000.
- [9] J. Blumenthal, F. Reichenbach, and D. Timmermann, "Position Estimation in Ad Hoc Wireless Sensor Networks with Low Complexity," *Proc. IEEE Workshop Positioning, Navigation, and Comm.*, pp. 41-49, Mar. 2005.
- [10] D. Niculescu and B. Nath, "Ad Hoc Positioning System (APS)," *Proc. Global Telecomm. Conf. (Globecom '01)*, vol. 1, pp. 2926-2931, Nov. 2001.
- [11] D. Niculescu and B. Nath, "DV Based Positioning in Ad Hoc Networks," *J. Telecomm. Systems*, vol. 22, pp. 267-280, Jan.-Apr. 2003.
- [12] X. Li, H. Shi, and Y. Shang, "A Partial-Range-Aware Localization Algorithm for Ad-Hoc Wireless Sensor Networks," *Proc. IEEE Int'l Conf. Local Computer Networks*, pp. 77-83, Aug. 2004.
- [13] T. He, C. Huang, B.M. Blum, J.A. Stankovic, and T. Abdelzher, "Range-Free Localization Schemes for Large Scale Sensor Networks," *Proc. ACM MobiCom '03*, pp. 81-95, Sept. 2003.
- [14] L. Doherty, K.S.J. Pister, and L.E. Ghaoui, "Convex Position Estimation in Wireless Sensor Networks," *Proc. IEEE INFOCOM '01*, vol. 3, pp. 1655-1663, Apr. 2001.
- [15] A. Galstyan, B. Krishnamachari, S. Patten, and K. Lerman, "Distributed Online Localization in Sensor Networks Using a Moving Target," *Proc. Int'l Symp. Information Processing in Sensor Networks*, pp. 61-70, Apr. 2004.
- [16] J. Hightower and G. Borriello, "Location Systems for Ubiquitous Computing," *Computer*, vol. 34, no. 8, pp. 57-66, Aug. 2001.
- [17] G.M. Djuknic and R.E. Richton, "Geolocation and Assisted GPS," *Computer*, vol. 34, no. 2, pp. 123-125, Feb. 2001.
- [18] G.J. Pottie and W.J. Kaiser, "Wireless Integrated Network Sensors," *Comm. ACM*, vol. 43, no. 5, pp. 51-58, May 2000.
- [19] J.-P. Sheu, S.-C. Tu, and C.-H. Yu, "A Distributed Query Protocol in Wireless Sensor Networks," *Wireless Personal Comm.*, vol. 41, no. 4, pp. 449-464, June 2007.
- [20] J.-P. Sheu, J.-M. Li, and C.-S. Hsu, "A Distributed Location Estimating Algorithm for Wireless Sensor Networks," *Proc. Int'l Conf. Sensor Networks, Ubiquitous, and Trustworthy Computing (SUTC '06)*, vol. 1, pp. 218-225, June 2006.
- [21] L. Hu and D. Evans, "Localization for Mobile Sensor Networks," *Proc. ACM MobiCom '04*, pp. 45-47, Sept. 2004.
- [22] M. Rudafshani and S. Datta, "Localization in Wireless Sensor Networks," *Proc. Int'l Conf. Information Processing in Sensor Networks (IPSN '07)*, pp. 51-60, Apr. 2007.
- [23] A. Uchiyama, S. Fujii, K. Maeda, T. Umedu, H. Yamaguchi, and T. Higashino, "Ad-Hoc Localization in Urban District," *Proc. IEEE INFOCOM '07*, pp. 2306-2310, May 2007.
- [24] K. Whitehouse and D. Culler, "A Robustness Analysis of Multi-Hop Ranging-Based Localization Approximations," *Proc. Int'l Conf. Information Processing in Sensor Networks (IPSN '06)*, pp. 317-325, Apr. 2006.
- [25] R. Stoleru, P. Vicaire, T. He, and J.A. Stankovic, "StarDust: A Flexible Architecture for Passive Localization in Wireless Sensor Networks," *Proc. ACM Int'l Conf. Embedded Networked Sensor Systems (SenSys '06)*, pp. 57-70, Oct. 2006.
- [26] A. Basu, J. Gao, J.S.B. Mitchell, and G. Sabhnani, "Distributed Localization Using Noisy Distance and Angle Information," *Proc. ACM MobiHoc '06*, pp. 263-273, May 2006.



**Jang-Ping Sheu** received the BS degree in computer science from Tamkang University, Taiwan, R.O.C., in 1981 and the MS and PhD degrees in computer science from National Tsing Hua University, Taiwan, in 1983 and 1987, respectively. He was the chair of the Department of Computer Science and Information Engineering, National Central University from 1997 to 1999. He was the director of the Computer Center, National Central University, from 2003 to 2006. He is currently a chair professor of the Department of Computer Science, National Tsing Hua University. His current research interests include wireless communications and mobile computing. He was an associate editor for the *Journal of the Chinese Institute of Electrical Engineering*, the *Journal of Information Science and Engineering*, the *Journal of the Chinese Institute of Engineers*, and the *Journal of Internet Technology*. He is an associate editor for the *IEEE Transactions on Parallel and Distributed Systems*, the *International Journal of Ad Hoc and Ubiquitous Computing*, and the *International Journal of Sensor Networks*. He received the Distinguished Research Awards from the National Science Council of the Republic of China in 1993-1994, 1995-1996, and 1997-1998, the Distinguished Engineering Professor Award from the Chinese Institute of Engineers in 2003, the certificate of Distinguished Professorship from the National Central University in 2005, and the K.-T. Li Research Breakthrough Award from the Institute of Information and Computing Machinery in 2007. He is a senior member of the IEEE and a member of the ACM and the Phi Tau Phi Society.



**Pei-Chun Chen** received the master's degree in computer science and information engineering from the National Central University, Taiwan, R.O.C., in 2006. Her research interests include localization and time synchronization in wireless sensor networks.



**Chih-Shun Hsu** received the BS degree in computer education from the National Taiwan Normal University, Taiwan, R.O.C., in 1990, the MS degree in computer science from the National Taiwan University, Taiwan, in 1992, and the PhD degree in computer science from the National Central University, Taiwan, in 2004. He joined the faculty of the Department of Information Management, Nanya Institute of Technology, Taiwan, in 1996 as an instructor and has been an associate professor since August 2004. He became the chairman of the Department of Computer Science and Information Engineering, Nanya Institute of Technology, in August 2005. Since August 2006, he has been with the faculty of the Department of Information Management, Shih Hsin University, Taiwan, as an assistant professor. His current research interests include wireless communications and mobile computing.

► For more information on this or any other computing topic, please visit our Digital Library at [www.computer.org/publications/dlib](http://www.computer.org/publications/dlib).